AMERICAN SOCIETY FOR MICROBIOLOGY | Journal of Bacteriology®

RESEARCH ARTICLE

Pleiotropic Regulation of Virulence Genes in *Streptococcus mutans* by the Conserved Small Protein SprV

Manoharan Shankar, Mohammad S. Hossain,* Indranil Biswas

Department of Microbiology, Molecular Genetics and Immunology, University of Kansas Medical Center, Kansas City, Kansas, USA

ABSTRACT *Streptococcus mutans*, an oral pathogen associated with dental caries, colonizes tooth surfaces as polymicrobial biofilms known as dental plaque. *S. mutans* expresses several virulence factors that allow the organism to tolerate environmental fluctuations and compete with other microorganisms. We recently identified a small hypothetical protein (90 amino acids) essential for the normal growth of the bacterium. Inactivation of the gene, SMU.2137, encoding this protein caused a significant growth defect and loss of various virulence-associated functions. An *S. mutans* strain lacking this gene was more sensitive to acid, temperature, osmotic, oxidative, and DNA damage-inducing stresses. In addition, we observed an altered protein profile and defects in biofilm formation, bacteriocin production, and natural competence development, possibly due to the fitness defect associated with SMU.2137 deletion. Transcriptome sequencing revealed that nearly 20% of the *S. mutans* genes were differentially expressed upon SMU.2137 deletion, thereby suggesting a pleiotropic effect. Therefore, we have renamed this hitherto uncharacterized gene as *sprV* (streptococcal pleiotropic regulator of virulence). The transcript levels of several relevant genes in the *sprV* mutant corroborated the phenotypes observed upon *sprV* deletion. Owing to its highly conserved nature, inactivation of the *sprV* ortholog in *Streptococcus gordonii* also resulted in poor growth and defective UV tolerance and competence development as in the case of *S. mutans*. Our experiments suggest that SprV is functionally distinct from its homologs identified by structure and sequence homology. Nonetheless, our current work is aimed at understanding the importance of SprV in the *S. mutans* biology.

IMPORTANCE *Streptococcus mutans* employs several virulence factors and stress resistance mechanisms to colonize tooth surfaces and cause dental caries. Bacterial pathogenesis is generally controlled by regulators of fitness that are critical for successful disease establishment. Sometimes these regulators, which are potential targets for antimicrobials, are lost in the genomic context due to the lack of annotated homologs. This work outlines the regulatory impact of a small, highly conserved hypothetical protein, SprV, encoded by *S. mutans*. We show that SprV affects the transcript levels of various virulence factors required for normal growth, biofilm formation, stress tolerance, genetic competence, and bacteriocin production.

KEYWORDS pleiotropic regulator, *Streptococcus mutans*, bacteriocins, biofilms, global virulence, stress response

Received 8 December 2016 **Accepted** 30 January 2017

Accepted manuscript posted online 6 February 2017

Citation Shankar M, Hossain MS, Biswas I. 2017. Pleiotropic regulation of virulence genes in *Streptococcus mutans* by the conserved small protein SprV. J Bacteriol 199:e00847-16. https://doi.org/10.1128/JB.00847-16.

Editor George O'Toole, Geisel School of Medicine at Dartmouth

Address correspondence to Indranil Biswas, ibiswas@kumc.edu.

* Present address: Mohammad S. Hossain, Department of Genetic Engineering and Biotechnology, University of Dhaka, Dhaka, Bangladesh.

Streptococcus mutans expresses various stress tolerance mechanisms and virulence factors, which allow the organism to endure the detrimental oral environment, colonize tooth surfaces as dental plaque, and eventually cause caries by demineralization of the enamel (1). The coordinated expression of stress responsive and virulence-related genes is critical for the persistence of *S. mutans* in the oral environment that

leads to successful colonization. The expression of these genes is effectively controlled at the transcriptional level by various transcriptional regulators and two-component systems and at the posttranscriptional and posttranslational levels by small RNAs (sRNAs) and regulatory proteases, respectively (2–4). The interplay among the regulators that act on various pathways achieves a critical level of virulence factors that contributes to pathogenesis.

In this regulatory network, the role of small proteins has largely been ignored, possibly due to the assigned size limits of open reading frames (ORFs) during annotation and the lack of bioinformatics approaches to annotate these small proteins (5). However, in today's genomic age, several small proteins that were previously unknown have been identified and their functions have been determined (see reference 6 and references therein). Small proteins have been shown to play critical roles in bacterial fitness and virulence by affecting the regulatory network. A recent survey in *Pseudomonas putida* KT2440 identified 14 new small proteins, of which two (Fis and CysB) with transcription regulatory function were characterized (7). Posttranscriptionally, small proteins may influence gene expression by affecting cellular levels of mRNA or by impacting translation. For example, Hfq-like RNA chaperones, which are small RNA-binding proteins, mediate posttranscriptional sRNA-mRNA interactions and contribute to the increased or decreased translation of target mRNAs (8, 9). A small RNA-binding protein, CsrA, in coordination with its sRNA partners CsrB and CsrC, acts globally to influence virulence gene expression in *Escherichia coli* and *Salmonella* (10, 11). Another small RNA-binding protein in enteric bacteria, SmpB, maintains cellular homeostasis by recovering stalled ribosomes and contributes to the SsrA-mediated tagging of improperly synthesized polypeptide chains (12). Some presumed bacterial small RNAs also encode functional protein regulators. SgrS is a small RNA that affects the translation of the *ptsG* mRNA in an Hfq-dependent manner. However, recently, this RNA was found to encode a small protein, SgrT, which contributes to glucose-phosphate stress response collaboratively with SgrS (13).

In the case of Gram-positive bacteria, the role of small regulatory proteins in *Bacillus subtilis* fitness has been well documented (6). HPr, for example, is a small protein with kinase and phosphorylase activity that is essential for catabolite repression in *B. subtilis* (14). Sda, another small protein of *B. subtilis*, functions as a DNA replication checkpoint and inhibits the initiation of spore formation in response to defective DNA replication. Sda also plays a regulatory role posttranslationally. Degradation of Sda by the regulatory protease ClpP is essential to remove the inhibitory effect that Sda imposes on sporulation (15).

Bacterial uptake of iron is essential for bacterial fitness and pathogenesis. Therefore, this process is tightly regulated by Fur in several bacteria. In *B. subtilis*, the Fur-regulated FbpA, FbpB, and FbpC proteins, which are small and basic in nature, are also known to act as metal chaperones in the iron-sparing response of *B. subtilis* (16). Understandably, the diverse functions of small proteins have prompted refinement in the annotation of genomes, leading to the identification of more small proteins in other bacteria by exploration of their small proteomes (5). Our group previously explored the regulatory function of HLP, which is an immunogenic nucleoid-associated small protein that contributes to the virulence of *S. mutans* (17). Furthermore, the function of CopZ, a small copper chaperone protein, has been recently characterized in *S. mutans*. However, it is unclear how the deletion of CopZ affects biofilm formation and bacteriocin production (18).

As part of our ongoing efforts to understand the regulation of bacteriocin production in *S. mutans*, we screened a transposon insertion library to identify potential regulators. We identified several mutant clones with insertions in the SMU.2137 locus. SMU.2137 is predicted to code for a small hypothetical protein of 90 amino acids (19). Here, we show that SMU.2137 encodes a protein product that pleiotropically regulates virulence gene expression in *S. mutans*. We renamed SMU.2137 as the streptococcal pleiotropic regulator of virulence (SprV). This work was aimed at investigating the potential regulatory role of SprV in *S. mutans* biology.

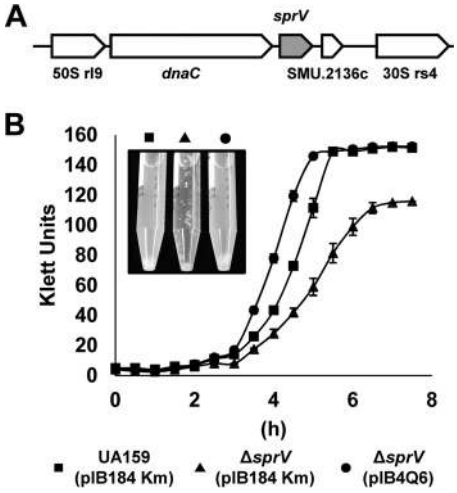

FIG 1 The *sprV* mutant suffers a growth defect and aggregates in liquid culture. (A) Organization of the genetic locus encoding SprV. Based on operon prediction tools, SprV, encoded by SMU.2137, appears to be expressed as part of an operon comprising SMU.2139c (encoding 50S ribosomal protein L9), SMU.2138c (*dnaC*), and SMU.2136c. However, a putative −10 box (TTCTAGTAT) and a putative −35 box (TTCCAA) are located within 60 bp upstream of the start codon of *sprV*. (B) Inactivation of *sprV* causes a growth defect and aggregated growth that is reversible upon in *trans* complementation of the mutation. All strains were grown in THY at 37°C in Klett flasks, and growth was monitored at 30-min intervals until the wild type reached the stationary phase. Growth curves were plotted using two replicates for each strain, and the experiment was repeated twice independently. The data shown are the means ± standard deviations from one such experiment.

RESULTS

***sprV* inactivation causes a growth defect and affects biofilm formation.** The SprV-encoding gene SMU.2137 (*sprV*) is predicted to be expressed as part of a four-gene operon encompassing SMU.2136c (encoding a hypothetical protein), SMU.2138c (encoding the replicative DNA helicase DnaC), and SMU.2139c (encoding 50S ribosomal protein L9) (20) (Fig. 1A). We noted that the *sprV* deletion mutant grew consistently slower than the wild-type parent on Todd-Hewitt medium–yeast extract (THY) agar and in THY broth during routine culturing, which prompted us to determine its growth kinetics. As shown in Fig. 1B, not only did the *sprV* mutant grow more slowly than the wild type, it also achieved a much lower final cell density (116 Klett units) than the wild-type strain (~150 Klett units). We determined the doubling time for each strain from the slope of the exponential growth phase. The parent strain and the complemented strain had doubling times of 44.26 ± 1.92 and 41.14 ± 0.78 min, respectively. The *sprV* mutant, however, had an extended doubling time of 62.77 ± 1.01 min, highlighting the growth defect it suffers as a result of *sprV* deletion. Furthermore, we also observed that the *sprV* mutant grew in clumps (Fig. 1B, inset) compared to the wild-type and complemented strains, suggesting increased cell-cell adhesion, possibly due to changes in its surface properties. Since cell-cell adhesion plays a key role in biofilm growth, we assessed the biofilm formation ability of the *sprV* mutant in the presence and absence of sucrose. Consistent with the observed increase in cell-cell adhesion, the *sprV* mutant formed better biofilms in THY than the wild-type and complemented strains on polystyrene 96-well plates. However, when 1% sucrose was added to THY, the mutant suffered a defect in biofilm formation compared with the wild-type and complemented strains (Fig. 2A). This effect was reproducible on glass as a biofilm substrate under similar conditions, as shown in the surface plots in Fig. 2B.

SprV is essential for stress tolerance response. Biofilms have been shown to be more tolerant to environmental stresses, suggesting a considerable regulatory overlap between biofilm formation and stress tolerance. Since the *sprV* mutant displayed altered biofilm-forming ability, we wanted to assess its ability to tolerate various environmental stresses. While the wild-type strain was tolerant of an acidic pH of 5.5,

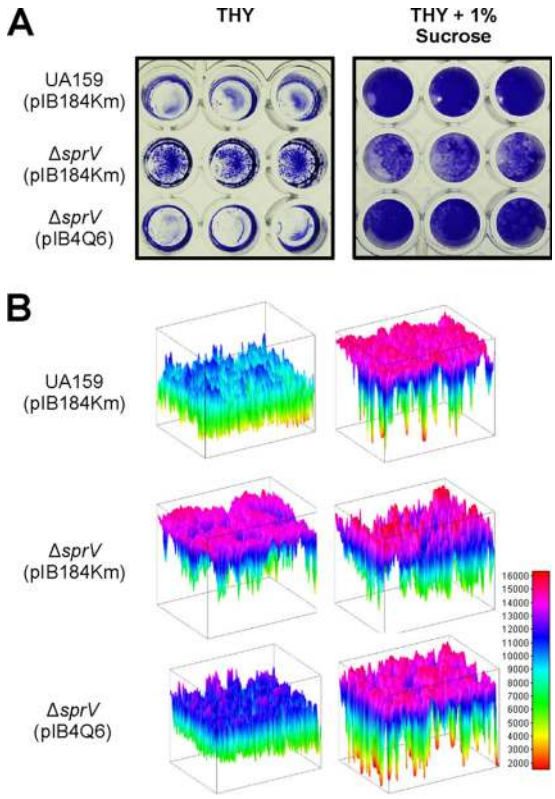

FIG 2 Loss of *sprV* function impacts sucrose-dependent and sucrose-independent biofilm formation in *S. mutans*. Cultures of strains to be tested were grown in 96-well microplates (A) or in chamber slides (B) to allow biofilm formation on polystyrene and glass as inert substrates. All strains were grown in THY or THY supplemented with 1% sucrose at 37°C for 48 h under microaerophilic conditions to allow biofilm formation in the presence or absence of sucrose, respectively. After sufficient growth, cultures were aspirated gently and wells were washed with PBS to remove planktonic cells, stained with crystal violet, washed to remove unbound dye, and then imaged. Images of biofilms grown on glass are rendered as surface plots using ImageJ for easy visualization. All biofilm formation assays were performed at least twice independently, and the data shown are from one such experiment.

a temperature of 42°C, and osmotic stress up to 0.5 M NaCl, the *sprV* mutant grew very poorly or failed to grow under these conditions (Fig. 3A to D). The mutant was also highly susceptible to oxidative stress induced by hydrogen peroxide and methyl viologen at concentrations that the wild type tolerated (Fig. 3E and F). Furthermore, exposure of the *sprV* deletion mutant to UV radiation for 15 s abolished growth (Fig. 3G), suggesting defects in UV-inducible DNA repair mechanisms. When complemented in *trans* with pIB4Q6, however, the *sprV* mutant was not susceptible to any of the above-listed stresses, indicating that the observed susceptibility is a result of *sprV* deletion. In addition, we noted that the *sprV* deletion strain was significantly more susceptible to killing by membrane-targeting peptide antibiotics (colistin and polymyxin B) and trimethoprim but that its susceptibility to other tested antibiotics was largely unaffected (Table 1).

The *sprV* mutant is defective for DNA uptake. Earlier work in our lab suggested that deletion of the SprV-encoding gene SMU.2137 may interfere with the uptake of linear DNA (19). We wanted to verify if this was true using plasmid DNA as well. We also assessed whether the addition of extraneous competence-stimulating peptide 18 (CSP-18) to the culture medium or increasing the transforming DNA concentration would alleviate the defect. The *sprV* deletion strain was barely transformable with 100 ng of pGhost9-TR in the presence of extraneous CSP-18. Increasing the plasmid level to 500 ng marginally increased transformability (Fig. 4B). The transformability of the *sprV* mutant in the presence of CSP-18 was comparable to the natural transformability of the wild type without extraneous CSP-18, suggesting that other factors in addition to

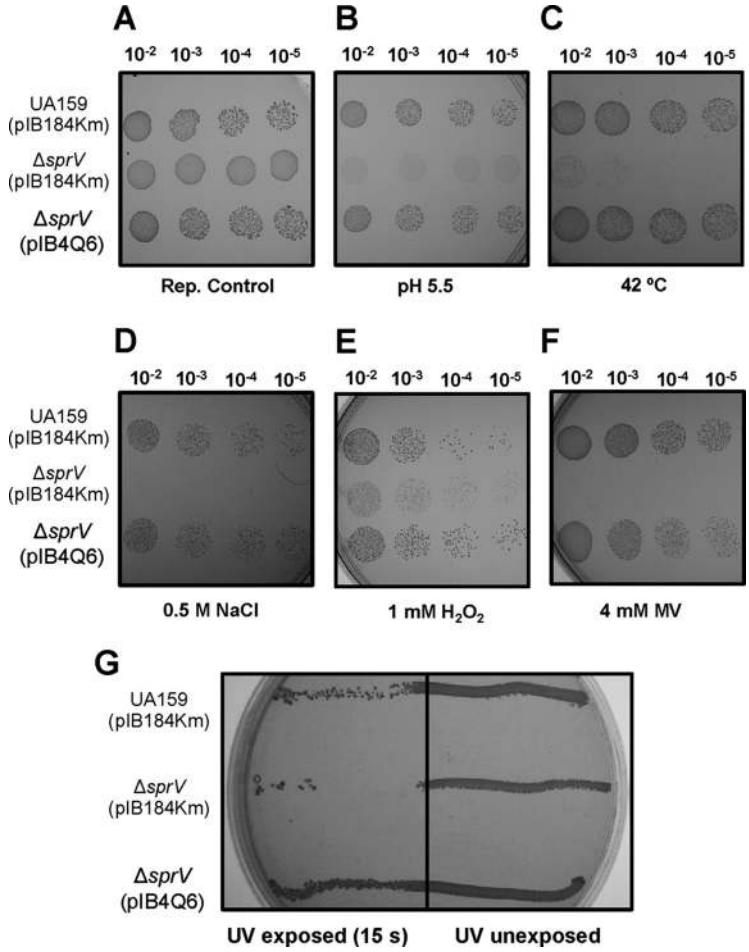

FIG 3 Deletion of *sprV* contributes to poor tolerance to acid, heat, osmotic, oxidative, and UV-induced stress. (A to F) THY plates containing various stressor compounds were prepared as detailed in Materials and Methods. Strains to be tested were first adjusted to similar cell densities and serially diluted. Aliquots of test strain dilutions were then spotted on THY agar (rep. control) and THY agar containing the indicated stressor compound or incubated under the indicated condition. MV, methyl viologen. (G) UV sensitivity was assessed by exposing half of the freshly swabbed bacterial culture on the THY agar surface to UV short-wave radiation for 15 s. Half of the plate was covered using a glass plate to block UV irradiation. All plates except the heat stress plate were incubated at 37°C under microaerophilic conditions, and growth was monitored for up to 72 h postinoculation. Heat stress plates were incubated at 42°C under microaerophilic conditions for up to 72 h. All stress tolerance assays were carried out thrice independently, and data shown are from one such experiment. Each stressor plate had its own control THY plate incubated under similar conditions. The data shown are from one such representative plate.

CSP-18 may be affected in the *sprV* deletion strain. In the absence of extraneous CSP-18, the *sprV* deletion mutant could not be transformed with either amount of pGhost9-TR, highlighting the severe defect in plasmid DNA uptake (Fig. 4B). However, when complemented in *trans* with pIB4Q6, the deletion mutant was transformable at levels similar to the wild-type strain (Fig. 4) irrespective of CSP-18 or plasmid DNA concentrations.

SprV pleiotropically regulates ~20% of the *S. mutans* genome. The deletion of *sprV* resulted in defective growth and various other defects that affect virulence. This led us to suspect that SprV may have a global effect on *S. mutans* gene expression. We performed a transcriptome profiling experiment by sequencing enriched mRNAs isolated from exponential-growth-phase cultures of *S. mutans* and its isogenic *sprV* mutant. Data analysis to identify differentially expressed genes (DEGs) revealed that 368 genes (~19% of the total of 1,960 protein-encoding genes) were at least 2-fold differentially expressed with an adjusted *P* value of <0.05 (Fig. 5). Of these 368 genes,

TABLE 1 Antibiotic and stress susceptibility of the *S. mutans sprV* mutant[a]

Stressor or antibiotic (concn)	Diam (mm) of zone of inhibition for:		
	UA159(pIB184Km)	Δ*sprV*(pIB184Km) mutant	Δ*sprV*(pIB4Q6) mutant
Stressors			
SDS (750 μg)	19.75 ± 1.06	23.25 ± 1.76	20.25 ± 1.06
2,2-Bipyridyl (780 μg)	13.25 ± 1.76	13.5 ± 1.41	12 ± 2.12
Antibiotics			
Colistin (200 μg)	8 ± 0	12.25 ± 1.06[b]	9.25 ± 0.35
Polymyxin B (200 μg)	10.25 ± 0.35	14 ± 0.70[b]	11.5 ± 0
Trimethoprim (5 μg)	13.5 ± 0.70	20.25 ± 1.06[b]	14.75 ± 0.35
Vancomycin (5 μg)	13 ± 0.70	14.75 ± 1.70	13.5 ± 0
Streptonigrin (1 μg)	25 ± 1.41	27.5 ± 0.70	23.75 ± 0.35

[a]All disc diffusion assays were conducted twice independently, and the data shown indicate the mean ± standard deviation.
[b]Signficantly different ($P < 0.05$) from the result for the wild type as calculated by Student's *t* test.

173 genes (47%) were upregulated (Fig. 5A) while 195 genes (53%) were downregulated (Fig. 5B). Considering the total number of protein-encoding genes in *S. mutans*, ~9% of genes were upregulated while ~10% of genes were downregulated, highlighting the pleiotropic nature of SprV's function. Even though the *sprV* mutant was

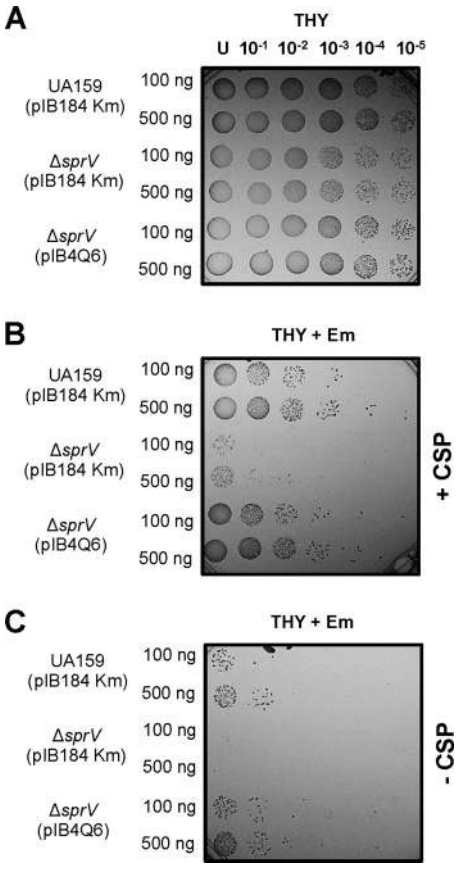

FIG 4 The *S. mutans sprV* mutant is defective for natural competence. Viability and natural competence of test strains were assessed in the presence and absence of competence-stimulating peptide (CSP-18). Typically, strains were cultured in THY containing horse serum until they reached exponential growth phase. As required, CSP-18 was added to these cultures, and the cultures were further incubated for 30 min, after which 100 ng or 500 ng pGhost-9TR (Em^r) was added to 1-ml aliquots of CSP-18-treated and CSP-18-untreated cultures. After additional incubation for 1 h, serial dilutions of the transformation mixes were made and aliquots of the dilutions were replicated by spotting on THY and THY containing erythromycin (Em). Competence assays were carried out twice independently, and the data shown are from one such experiment.

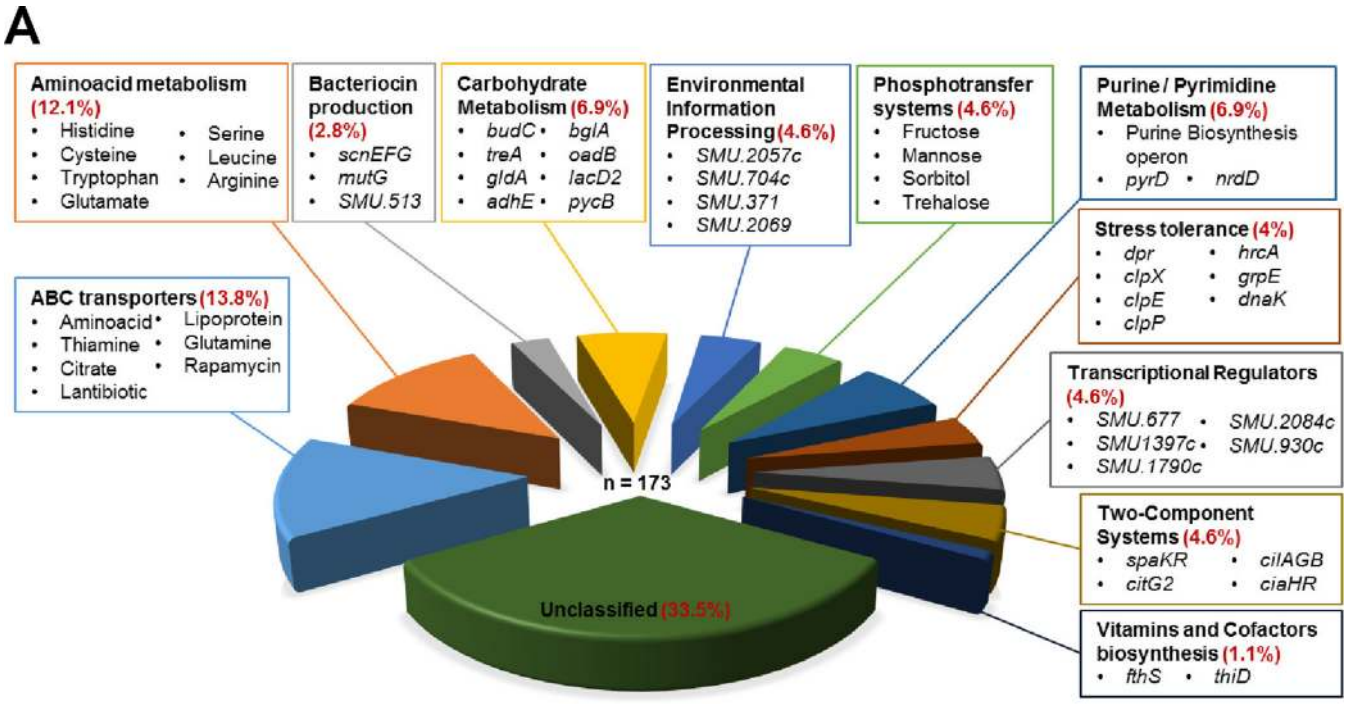

FIG 5 The *sprV* gene product pleiotropically regulates several classes of genes contributing to virulence and stress tolerance. Classification of genes increased (A) or decreased (B) in expression upon loss of SprV. Genes that were at least 2-fold differentially expressed with a significance value of <0.05 were grouped based on their KEGG classification. A few important genes/functions from each functional class are highlighted. Of a total of 368 genes that were differentially expressed, 173 genes (ATP-dependent transport, amino acid metabolism, carbohydrate metabolism, and nucleotide metabolism genes) were upregulated as a result of SprV loss. Around 195 genes (stress tolerance, environmental information processing, nucleic acid metabolism, and transcriptional regulation genes) were downregulated upon *sprV* deletion.

defective for bacteriocin biosynthesis, bacteriocin immunity genes (*scnE*, *scnF*, and *scnG*) and the lantibiotic protection ABC transporter permease gene (*mutG*) were upregulated. Several heat shock responsive genes (*hrcA*, *grpE*, and *dnaK*) were upregulated in the *sprV* mutant, indicating that the mutant suffered some stress as a result of the *sprV* deletion. In addition, *dpr*, which is a *dps*-like peroxide resistance gene, was

upregulated in the mutant. The genes coding for the peptidase (*clpP*) and ATPase (*clpX* and *clpE*) components of the Clp protease were upregulated in the *sprV* mutant. Moreover, genes encoding the CiaHR and SpaKR two-component systems, involved in the regulation of competence and resistance to the polycyclic antibacterial peptide nisin, respectively, were upregulated in the *sprV* mutant. Around 58 genes could not be classified into any of the functional categories and formed ~33.5% of the total upregulated genes. Similarly, around 44.6% of the downregulated genes (87) could not be classified into the above-mentioned categories. Consistent with the *sprV* mutant's observed defect in bacteriocin production, several bacteriocin production (*nlmAB*, *nlmC*, and *nlmD*) and immunity genes were downregulated. The competence-stimulating peptide-encoding gene *comC* was downregulated 5-fold upon *sprV* deletion and may contribute to the severe defect in natural competence. Genes encoding the primary adhesin of *S. mutans*, SpaP, and the sortase enzyme required for its anchoring (SrtA) were upregulated by 1.4- and 1.7-fold, respectively, in the *sprV* deletion mutant. The *sloC* gene coding for the lipoprotein receptor antigen (LraI) class adhesin was also upregulated. The gene encoding a glucosyl transferase (*gtfB*) that is critical for sucrose-dependent glucan biosynthesis was downregulated by 2.6-fold upon *sprV* deletion. In addition, *gbpA*, *gbpB*, and *gbpC*, coding for glucan-binding proteins, were downregulated by 2.4-, 1.7-, and 2.6-fold, respectively. Although several heat shock responsive genes were upregulated in the *sprV* mutant, the *groEL* and *groES* chaperone system-encoding genes were downregulated. Genes encoding an osmoprotectant ABC transporter system (*opuCA*, *opuCB*, *opuCC*, and *opuCD*) were downregulated in the *sprV* mutant. Several genes that are involved in DNA replication (*holB*, *mutY*, and *polI*) and in DNA repair (*uvrA*, *trcF*, and *recN*) were downregulated upon *sprV* inactivation. The VicRK two-component system, which has been implicated in biofilm formation, tolerance to various stresses, and expression of virulence factors, was the only prominent two-component system that was 2-fold downregulated upon *sprV* deletion. Multiple transcriptional regulators, such as the purine operon repressor (*purR*), the regulator of multiple-sugar metabolism (*msmR*), and the virulence regulator *brpA*, were downregulated in the *sprV* mutant. *dfrA*, which encodes dihydrofolate reductase, an enzyme required for resistance to trimethoprim, was downregulated upon *sprV* inactivation. Moreover, *dltA*, *dltB*, and *dltD*, which are involved in D-alanylation of lipoteichoic acid (LTA), were downregulated by 1.75-, 1.75-, and 1.6-fold, respectively. D-Alanylation of LTA is known to impact aggregation, autolysis, biofilm formation, acid resistance, and susceptibility to antimicrobial peptides. Among other stress tolerance genes, those encoding the ATPases ClpB and ClpC and penicillin-binding proteins (Pbp2a and Pbp1a) were notably downregulated.

SprV also affects the *S. mutans* proteome. Since we found that SprV affects the expression of several key virulence factors and since we suspected a wide regulatory role for SprV, we compared the protein profile of the *sprV* mutant with that of the wild type. Tris-Tricine SDS-PAGE revealed that the *sprV* mutant had an altered protein profile compared with the wild type. When the mutant was complemented in *trans* with pIB4Q6, the wild-type-like protein profile was restored (Fig. 6). We found that eight proteins in the mutant were differentially expressed compared with those in the wild type (Fig. 6, arrowheads). Of these, the prominently upregulated protein band, slightly above the 15-kDa standard (Fig. 6, lowest arrowhead), was identified as Dpr, which is a peroxide resistance protein.

SprV contains a highly conserved Veg domain and a motif structurally similar to Hfq. To get insights into the expression levels of the *sprV* gene product, we assessed the *sprV* transcript and protein levels in the *S. mutans* wild-type strain. Semiquantitative reverse transcriptase PCR (sq-RT-PCR) revealed that the *sprV* transcript was expressed constantly throughout the growth phases (Fig. 7A). However, our attempts to detect SprV in clarified cell lysates of the wild type by immunoblotting were unsuccessful (Fig. 7B). Therefore, we attempted to determine if SprV localized to the cell surface or was secreted into the culture medium. We observed that a protein band of ~10 kDa was

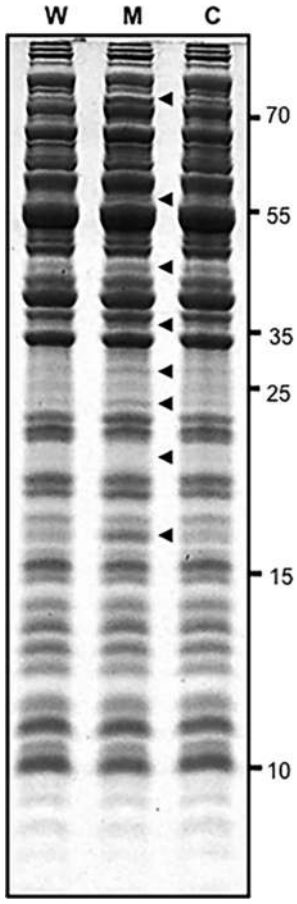

FIG 6 The SprV mutant displays an altered protein profile. The protein profile of test strains was obtained by SDS-PAGE of their cell lysates obtained by mechanical disruption and clarified by centrifugation. Protein samples were quantified, and equal amounts were loaded onto each lane. Differentially expressed protein bands are highlighted with arrowheads, and molecular weight markers are indicated on the right. The samples are as follows: W, *S. mutans* UA159; M, *S. mutans* Δ*sprV*; C, *S. mutans* Δ*sprV* complemented with pIB4Q6.

present in the pellet fraction of the wild-type strain but was absent in the *sprV* mutant (Fig. 7B). No such difference was observable in the proteins precipitated by trichloroacetic acid (TCA) from the spent culture medium (data not shown) or the cell wall proteins (Fig. 7B).

Analysis of the SprV amino acid sequence indicated that a Veg-like domain (PF06257) spanned between positions 9 and 87 of the protein (Fig. 7C). We predicted the secondary structure of SprV and found that the protein folded to form an N-terminal α-helix followed by five β-sheets spanning the protein. A short α-helix was present between positions 76 and 79 in the sequence. Except the variable loop region between β-sheets 3 and 4, the entire protein was extremely well conserved among all streptococci (Fig. 7C and D). SprV contained a short stretch of positively charged amino acids (RKR) in the loop region between β-sheets 1 and 2, which was predicted to bind nucleic acids (21). However, RKR→AAA mutation did not abolish the *in vivo* activity of SprV (data not shown). Sequence comparison between *S. mutans* SprV and its homolog in *Streptococcus pneumoniae* also displayed a primary sequence identity of ~73%. This SprV homolog in *S. pneumoniae* was predicted to interact with ribosomal protein L9 in a proteome-wide interaction screen for unannotated proteins (22). Moreover, we noted that the *S. mutans* ribosomal protein S2 copurifies with SprV-6×His (data not shown). To test whether SprV interacts with its potential interaction partners L9 and S2, we performed a bacterial two-hybrid assay. SprV was unable to interact with ribosomal proteins L9 and S2 (Fig. 8A). However, SprV was found to oligomerize *in vivo* (Fig. 8A).

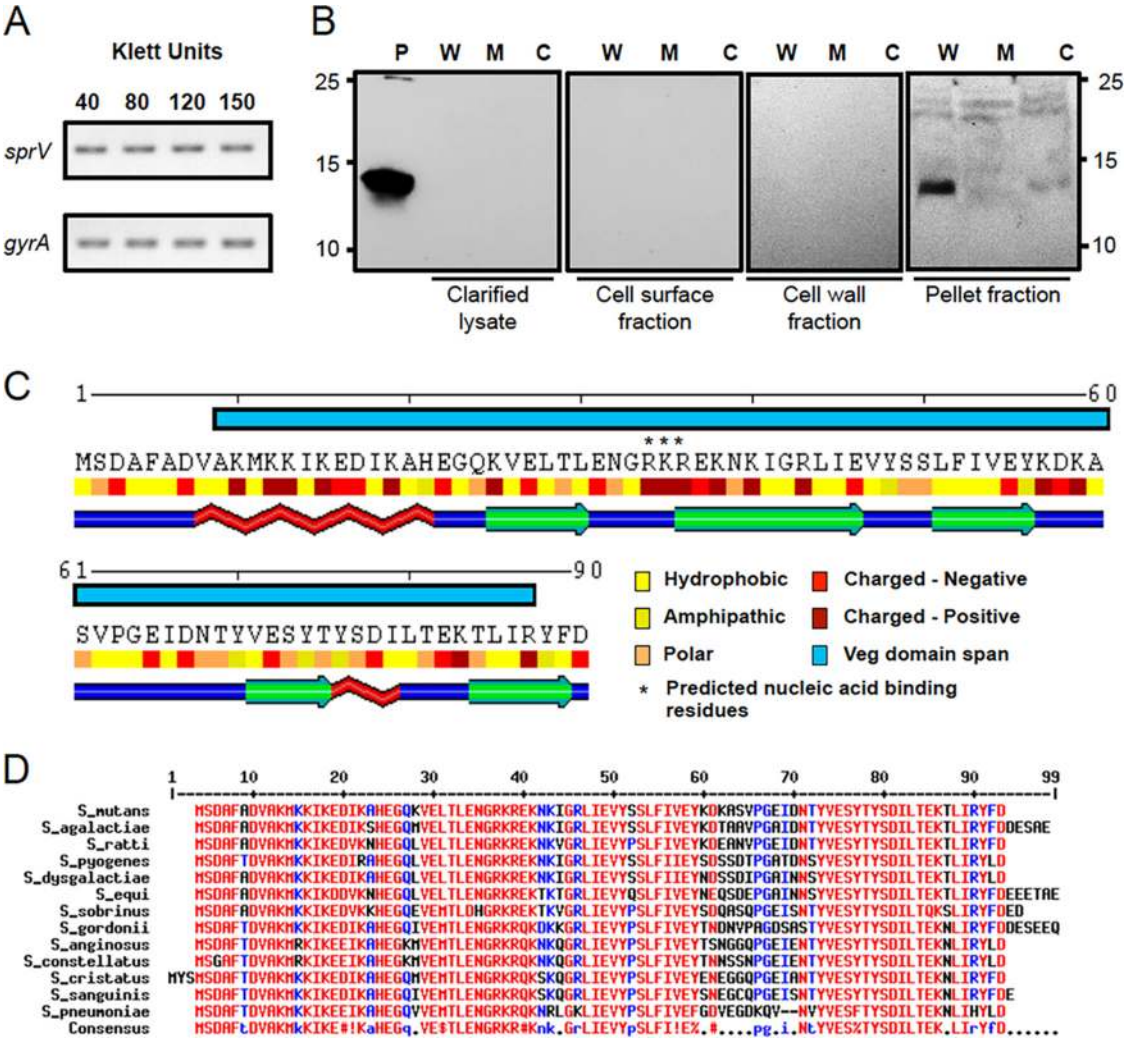

FIG 7 *sprV* encodes a highly conserved Veg domain-containing protein that is actively transcribed yet poorly detectable by immunoblotting. (A) Levels of *sprV* transcript were determined by semiquantitative reverse transcription-PCR from RNA obtained from *S. mutans* UA159 cultures at various growth phases (40 Klett units, early log phase; 80 Klett units, mid-log phase; 120 Klett units, late log phase; 150 Klett units, stationary phase). (B) Immunoblotting for detection of SprV in the subcellular fractions of test strains was carried out using an anti-SprV peptide antibody as the primary antibody and an anti-rabbit IgG–HRP conjugate as the secondary antibody. Bands were detected using the ECL Plus chemiluminescent detection substrate and imaged by exposure to X-ray film. Cell lysate, cell surface, cell wall, and pellet fractions were prepared from exponential-growth-phase cultures of the wild type (W), *sprV* mutant (M), and *sprV* mutant complemented with in *trans sprV* (C) as detailed in Materials and Methods. Purified SprV (P) was used as a positive control for the immunoblotting experiment. (C) Schematic representation of the SprV protein indicating amino acid characteristics, span of the Veg domain, predicted secondary structure, and predicted nucleic acid-binding residues. (D) Multiple-sequence alignment of SprV homologs from streptococci, indicating a high degree of sequence conservation and showing the variable loop region between β-sheets 3 and 4.

The crystal structure of the SprV homolog in *S. pneumoniae* (Protein Data Bank [PDB] accession number 3FB9) displayed a secondary structure similar to the predicted secondary structure of SprV. Using the 3FB9 structure as the template, the 3-dimensional structure of *S. mutans* SprV was modeled on the Phyre2 server (Fig. 8B). A structural homology search using the crystal structure of *S. pneumoniae* SprV (PDB accession number 3FB9) as input on the PDBeFold server identified two structures of the RNA chaperone Hfq from *Staphylococcus aureus* (PDB accession numbers 1KQ1 and 3QSU) (Fig. 8C) as the best hits, with root mean square deviation (RMSD) values of 2.25 and 2.3, respectively, and a query coverage of 86%. Therefore, we wanted to determine if in *trans sprV* expression could cross-complement an *E. coli hfq* deletion mutant. We expressed SprV fused to an N-terminal histidine tag from pIB190 and in its native form from pIB184Em in an *E. coli hfq* mutant containing an *rpoS-lacZ* fusion. We checked the

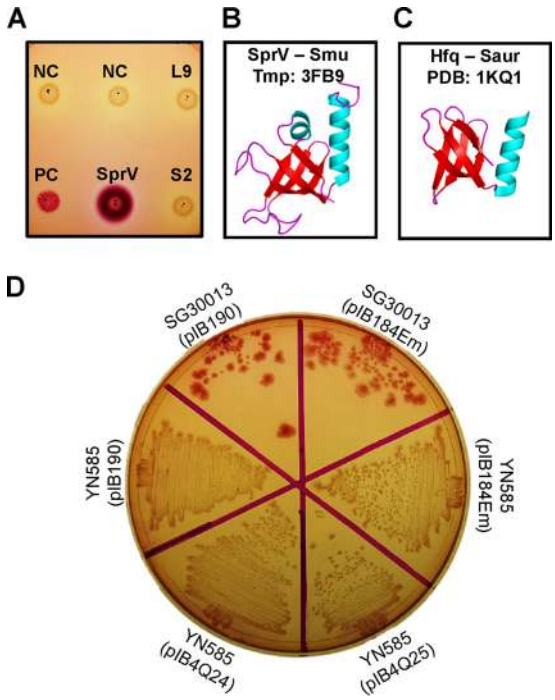

FIG 8 SprV is structurally similar to the RNA chaperone Hfq but cannot functionally replace Hfq in an *E. coli* Δ*hfq* mutant. (A) Bacterial two-hybrid assay to assess the interaction between SprV and its predicted interaction partners. NC, *E. coli* BHT101(pKT25, pUT18); PC, *E. coli* BHT101(pKT25-zip, pUT18C-zip); L9, *E. coli* BHT101(pIB4Q45, pIB4Q48); S2, *E. coli* BHT101(pIB4Q45, pIB4Q47); SprV, *E. coli* BHT101(pIB4Q45, pIB4Q46). (B) A three-dimensional model of SprV was predicted on the Phyre2 server using the crystal structure of the SprV homolog from *S. pneumoniae* TIGR4 as the template. (C) The crystal structure of the RNA chaperone Hfq monomer from *Staphylococcus aureus* (PDB accession number 1KQ1), which was identified as a structural homolog of *S. pneumoniae* SprV by the PDBeFold server. (D) *rpoS-lacZ* fusion expression was assessed on MacConkey agar in the *E. coli* wild type (SG30013) and in the *E. coli hfq* deletion mutant containing an *rpoS-lacZ* fusion (YN585) when SprV was expressed in *trans* from vectors pIB190 and pIB184Em. Appropriate vector controls are indicated.

expression of SprV in *E. coli* using immunoblotting (data not shown). However, neither the His-tagged SprV nor its native form could functionally replace Hfq in *E. coli* YN585 by inducing expression of the Hfq-dependent *rpoS-lacZ* fusion, as indicated by white colonies on MacConkey agar (Fig. 8D).

Inactivation of *sprV* in *Streptococcus gordonii* also causes defects in DNA uptake and UV resistance and an altered protein profile. Since SprV was highly conserved across streptococci, we inactivated the *sprV* homolog in *S. gordonii* (SGO_0029) to determine whether the *S. gordonii sprV* mutant would suffer defects as observed in *S. mutans*. As in *S. mutans*, loss of SprV in *S. gordonii* rendered the mutant sensitive to UV-induced damage (Fig. 9A). Furthermore, the *S. gordonii sprV* mutant suffered a marked defect in natural competence, comparable to that seen in *S. mutans* (Fig. 9B). Similarly, the *S. gordonii sprV* mutant also displayed an altered protein profile as observed by SDS-PAGE (Fig. 9E). However, when the *S. gordonii sprV* gene was introduced in *trans*, it was able to reverse the effects of *sprV* deletion. Since the homologs showed a considerable level of sequence similarity, we also attempted to cross-complement the *S. mutans sprV* deletion with the *S. gordonii sprV* gene expressed in *trans*. *S. gordonii sprV* was able to fully complement the *S. mutans sprV* mutant, as shown by the complete reversal of defects in UV tolerance and natural competence development (Fig. 9C and D). Furthermore, expression of *S. gordonii* SprV in the *S. mutans sprV* mutant restored a wild-type-like protein profile in the mutant (Fig. 9E). Surprisingly, *S. mutans sprV* only partially complemented the *sprV* deletion in *S. gordonii* (data not shown).

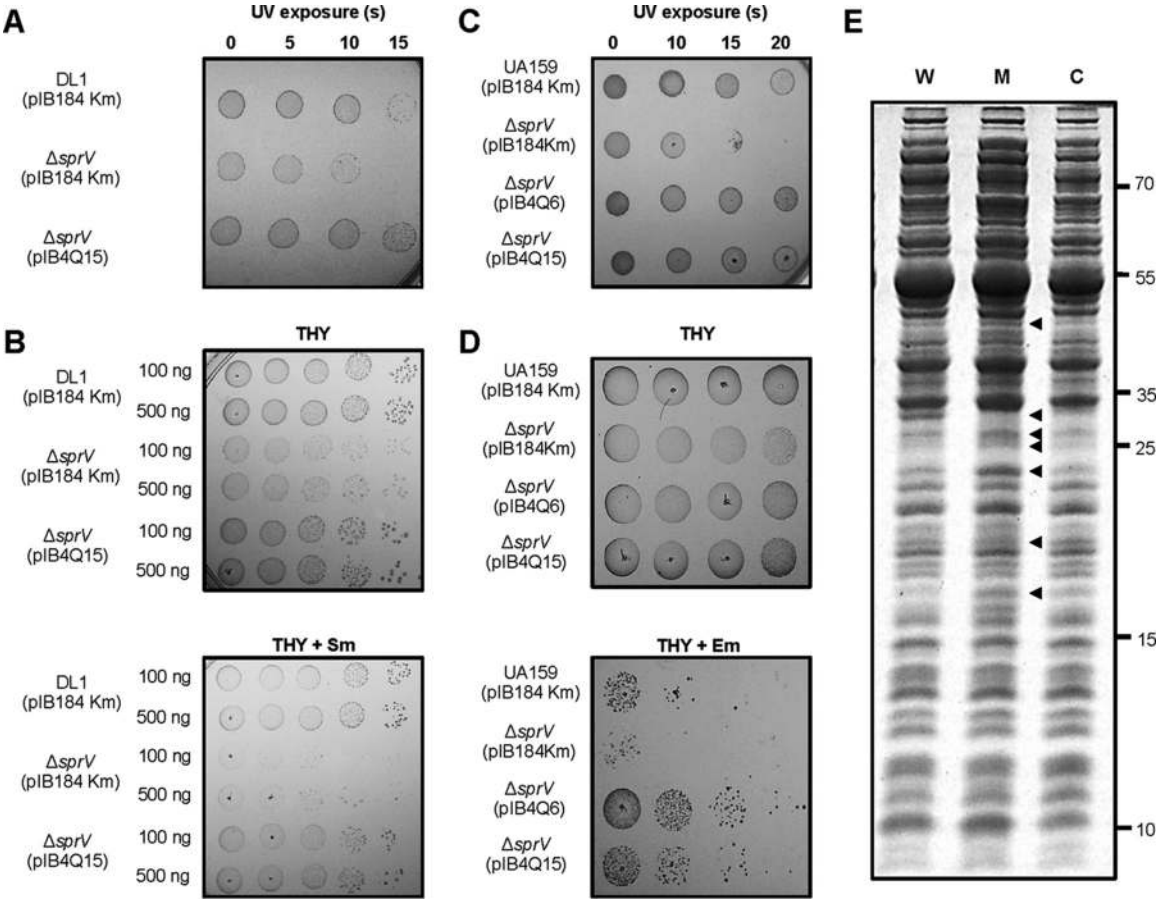

FIG 9 Inactivation of the *sprV* ortholog in *S. gordonii* leads to defective UV tolerance and natural competence and an altered protein profile. (A) UV sensitivities of *S. gordonii* wild-type DL1, its isogenic Δ*sprV* derivative, and the in *trans* complemented Δ*sprV* strain were assessed by spotting cell suspensions of test strains with identical cell densities on THY agar and exposing spots to various time intervals (0 to 15 s) of short-wave UV radiation. Regions of the plate to be protected from UV were covered with a glass plate. (B) Natural competence of *S. gordonii* strains was assessed as described in the legend to Fig. 4, except that CSP-18 was not used in this experiment, genomic DNA of a streptomycin-resistant derivative of *S. gordonii* DL1 was used to transform test strains, and transformants were selected for streptomycin resistance. (C) UV sensitivities of the *S. mutans* wild type, its isogenic Δ*sprV* derivative, the Δ*sprV* strain complemented in *trans* with *S. mutans sprV*, and the *S. mutans* Δ*sprV* strain complemented with *S. gordonii sprV* were assessed as described above. (D) Genetic competence of the *S. mutans* Δ*sprV* strain cross-complemented with *sprV* from *S. gordonii* was determined in comparison with wild-type *S. mutans*, its isogenic Δ*sprV* mutant, and the Δ*sprV* mutant complemented with *S. mutans sprV*. (E) Protein profile of *S. gordonii* DL1 and its derivatives. Experiments were done as described in the legend to Fig. 6. Differentially expressed protein bands are highlighted with arrowheads, and the molecular weight markers are indicated. The samples are as follows: W, *S. gordonii* DL1; M, isogenic Δ*sprV* mutant; C, Δ*sprV* mutant complemented with pIB4Q15.

DISCUSSION

SprV was originally identified as a potential regulator of mutacin production and genetic competence in *S. mutans* (19). However, the increased doubling time and lower final cell density that we observed upon *sprV* inactivation suggested a much larger role for SprV in the physiology of the organism. SprV is highly conserved in all streptococci, with homologs in other Gram-positive bacteria that are annotated as the Veg protein. At the sequence level, SprV contains a single conserved Veg domain (PF06257) belonging to the DUF1021 superfamily, which spans the majority of the protein sequence. In *B. subtilis* 168, deletion of *veg* had no effect on the growth rate of the strain (23), which is in contrast with the considerable growth defect that *S. mutans* suffers upon *sprV* inactivation (Fig. 1B). Overproduction of the Veg protein in *B. subtilis* 168 has been reported to promote biofilm formation by impacting the transcription of the *tapA-sipW-tasA* operon, which is involved in the synthesis of the extracellular matrix component of biofilms. This is achieved by inhibition of the master repressor SinR, although it is unclear how this inhibition occurs (23). Deletion of the *veg* homolog *sprV* in *S. mutans*, however, led to aggregation during growth (Fig. 1B) and enhanced biofilm

formation in the absence of sucrose (Fig. 2). Conversely, the sucrose-dependent pathway for biofilm formation appeared to be downregulated, as the *sprV* mutant formed poorly developed biofilms during growth in THY containing sucrose (Fig. 2). This dysregulation of the biofilm formation pathway in *S. mutans* suggested the differential expression of several genes of the pathway upon *sprV* inactivation. Several factors that affect biofilm formation in *S. mutans* are also known to impact its ability to tolerate environmental stresses and uptake DNA naturally (18, 24–26). As expected, our experiments showed not only that the *sprV* mutant was susceptible to various stresses and antibiotics (Fig. 3 and Table 1) but also that it was severely defective in DNA uptake (Fig. 4A). These findings, taken together with variations in the protein profile of the *sprV* mutant (Fig. 6), suggested a more significant role for SprV in the cell than we previously expected.

Transcriptome sequencing confirmed that SprV modulates the mRNA levels of nearly 368 genes of *S. mutans* in a pleiotropic manner (Fig. 5). This broad impact of SprV on cellular homeostasis may be due partly to the differential expression of several regulatory proteins. For example, *comC*, which is one of the highly downregulated genes upon loss of *sprV*, encodes the CSP that is involved not only in the development of competence but also in bacteriocin production and biofilm formation (24, 27). Loss of *brpA*, which is downregulated in the *sprV* mutant, results in the differential expression of ~200 genes and affects biofilm formation, acid tolerance, and the oxidative stress tolerance ability of *S. mutans* (26). VicRK, a two-component system, is downregulated upon *sprV* inactivation and is involved in the regulation of glucosyl transferases and glucan-binding proteins that are instrumental for sucrose-dependent biofilm formation (25). Moreover, the VicRK system is also reported to be involved in tolerance to oxidative stress and the development of genetic competence (28). The CiaHR two-component system, which is upregulated upon *sprV* deletion, has been shown to be involved in biofilm formation, acid tolerance, genetic competence, and the expression of the stress-responsive protease HtrA (29). Similarly, the heat shock responsive transcriptional repressor HrcA, which is upregulated in the *sprV* mutant, also affects acid tolerance by affecting levels of cellular chaperones (30). Loss of SprV causes an increase in the transcript levels of *clpP*. Our laboratory has previously shown that ClpP is involved in mutacin production, antibiotic stress tolerance, and control of gene expression from TnSmu1 and TnSmu2 genomic islands (31). Although our transcriptomic data aligned with the observed phenotypes, it was impossible to predict how SprV affects gene expression because of the largely interconnected pathways affecting these cellular processes.

Following a different approach, we tried to find out how SprV affects gene expression. We attempted unsuccessfully to detect SprV in the clarified cell lysate of *S. mutans* UA159 by immunoblotting using a custom-developed peptide antibody raised in rabbits, although a few nanograms of purified SprV-6×His were easily detectable (Fig. 7B). Since a similar observation was made in *B. subtilis*, wherein the Veg protein was undetectable by immunoblotting, we assessed the transcript levels of *sprV* in RNA samples prepared from cultures fixed at the early, mid-log, late log, and stationary growth phases. In accordance with the observations made with Veg from *B. subtilis* (23, 32), the *sprV* transcript was detectable at consistent levels throughout the growth phases of *S. mutans*, while the protein could not be detected from cell lysates prepared from cells at the exponential growth phase (Fig. 7). We reasoned that the protein may be secreted outside the cell despite lacking an *in silico* predictable signal peptide or that it may localize to the cell surface. Interestingly, an SprV homolog in *Streptococcus oralis* was detected in the cell surface-associated fraction prepared by extraction of surface proteins with *N*-dodecyl-*N*,*N*-dimethyl-3-ammonio-1-propanesulfonate (33). However, our attempts to detect SprV in cell surface and cell wall extracts of *S. mutans* (Fig. 7) and in TCA-precipitated proteins from cell-free culture supernatants (data not shown) were not successful. This observation led us to suspect that *sprV* codes for a regulatory RNA molecule as in the case of *sgrS* in *E. coli* (13). It was proved otherwise when we determined that pIB4Q34, which contains the *sprV* ORF with a frameshift

mutation in the start codon of the ORF (ATG→ATAG), could not complement the Δ*sprV* mutation (data not shown). As a final resort, we assessed by immunoblotting to see whether SprV could be detected by analysis of concentrated SDS extracts of the pellet obtained after cell lysis by mechanical disruption. We obtained a weak yet clear band between 10 and 15 kDa in the wild-type strain and in the in *trans* complemented strain, which was completely absent in the Δ*sprV* strain, thereby confirming that SprV was expressed in the cell and localized to the pellet fraction after lysis (Fig. 7B).

SprV is highly conserved across streptococci. Inactivation of the *sprV* homolog in *S. gordonii* resulted in sensitivity to UV, defective DNA uptake, and an altered protein profile, as in the case of *S. mutans*. Furthermore, the *sprV* homolog from *S. gordonii* could cross-complement an *S. mutans sprV* mutant, indicating the high degree of conservation of SprV. Closer sequence analysis of SprV indicated a highly conserved stretch of positively charged amino acids in the loop region between β-sheets 1 and 2, which was predicted to bind nucleic acids using BindN (21). Mutation of these residues to alanine did not affect the ability of SprV RKR→AAA to complement an *sprV* mutant, indicating that these residues were not critical to the function of SprV in the cell (data not shown). The structure of the SprV homolog from *S. pneumoniae* was solved earlier as part of a structural genomics study (PDB accession number 3FB9). As mentioned before, this structure shares a significant degree of homology with the structure of the RNA chaperone Hfq from *Staphylococcus aureus* (PDB accession number 1KQ1). Loss of *hfq* in several bacteria has led to the pleiotropic dysregulation of gene expression and susceptibility to various stresses in Gram-negative bacteria (34). In Gram-positive bacteria, loss of *hfq* sometimes perturbs normal cellular function, as in the case of *Listeria monocytogenes* (35), whereas it appears to have no effect in other cases, such as in *S. aureus* (36). Given the phenotypes that we observed for *sprV* deletion and the pleiotropic impact that SprV has on gene expression, we wanted to test whether SprV may be the elusive Hfq homolog in streptococci. Despite the structural homology, SprV was unable to complement an *E. coli hfq* mutant and induce expression of the *rpoS-lacZ* fusion that the strain harbors. Furthermore, purified SprV did not exhibit ATPase activity and it could not bind ATP (data not shown), which are both typical of Hfq. SprV also lacks the signature Sm domain that is characteristic of Hfq proteins (37). Collectively, these observations indicated that although SprV and Hfq have similar structures, they may be functionally distinct.

Using SprV-6×His, we attempted to pull down the interaction partners of SprV from *S. mutans* cell lysates. Ribosomal protein S2 was identified as a potential hit in one of these experiments (data not shown). Previously, in a proteome-wide protein interaction screen, the SprV homolog of *S. pneumoniae* SP2202 was reported to interact with ribosomal protein L9 (SP2204) (22). However, based on our bacterial two-hybrid assay, SprV was unable to interact with ribosomal proteins L9 and S2 (Fig. 8A). Currently, we have set up several experiments, including pull down and cross-linking approaches, to identify interacting partners of SprV and thereby further investigate the mysterious mechanism by which SprV widely impacts the *S. mutans* transcriptome.

MATERIALS AND METHODS

Bacterial strains and growth conditions. *S. mutans* strains were routinely grown in Todd-Hewitt medium (Becton Dickinson) supplemented with 0.2% yeast extract (THY) at 30°C or 37°C under microaerophilic conditions (i.e., in candle jars). Whenever needed, THY was supplemented with 5 μg/ml erythromycin (Em) and/or 300 μg/ml kanamycin (Km). *E. coli* strains were grown in Luria-Bertani medium that was supplemented with 100 μg/ml ampicillin (Ap), 50 μg/ml Km, 20 μg/ml chloramphenicol (Cm), or 500 μg/ml Em as required. To assess the growth kinetics of streptococci, overnight cultures of strains were diluted to equal densities (optical density at 600 nm [OD_{600}] = 0.05) in 50 ml of prewarmed THY contained in Klett flasks. Growth was monitored every 30 min using a Klett colorimeter with a red filter. Doubling time in minutes was calculated from the slope of the exponential growth phase of each strain.

Construction of bacterial strains and plasmids. Markerless gene deletions in *S. mutans* and *S. gordonii* were constructed by homologous recombination employing the Cre-*loxP* system for excision of the antibiotic resistance cassette as described earlier (38). The resulting strains were verified by sequencing the genomic loci for any secondary mutations. For in *trans* expression of *sprV* in streptococci, a shuttle expression vector, pIB184Km (39), was used. The *sprV* gene from *S. mutans*, along with its upstream elements (300 bp), was PCR amplified using primer pair 4Q2137CompF/4Q2137CompClonR (for all

TABLE 2 List of strains and plasmids used in this study

Strain or plasmid	Description	Reference or source
Strains		
S. mutans		
UA159	Wild type	46
Δ*sprV* mutant	Markerless deletion of SMU.2137	This study
Δ*sprV*(pIB4Q6) mutant	Markerless deletion of SMU.2137 complemented with SMU.2137	This study
Δ*sprV*(pIB4Q15) mutant	Markerless deletion of SMU.2137 complemented with *S. gordonii* 0029	This study
S. gordonii		
DL1	Wild type	47
Δ*sprV* mutant	Markerless deletion of 0029	This study
Δ*sprV*(pIB4Q15) mutant	Markerless deletion of 0029 complemented with *S. gordonii* 0029	This study
E. coli		
SG30013	MG1655 derivative with *rpoS-lacZ* fusion	44
YN585	SG30013 derivative; *hfq*::*cat* Cm^r	45
BHT101	F$^-$ *cya-99 araD139 galE15 galK16 rpsL1* (Str^r) *hsdR2 mcrA1 mcrB1*	48
Plasmids		
pGEMT-Ez	TA cloning vector; Ap^r	Promega
pIB184Km	*E. coli-Streptococcus* shuttle expression vector; Km^r	39
pIB184Em	*E. coli-Streptococcus* shuttle expression vector; Em^r	39
pIB190	*E. coli-Streptococcus* shuttle expression vector; Em^r	39
pET3a	Protein expression vector; Ap^r	Novagen
pKT25	Allows expression of protein as in-frame fusion at C terminus of T25 polypeptide; Km^r	48
pUT18	Allows expression of protein as in-frame fusion at N terminus of T18 polypeptide; Ap^r	48
pKT25-zip	Derivative of pKT25 with leucine zipper of GCN4 fused in frame to T25 polypeptide; Km^r	48
pUT18C-zip	Derivative of pUT18C with leucine zipper of GCN4 fused in frame to T18 polypeptide; Ap^r	48
pIB4Q6	pIB184Km containing SMU.2137 in reverse orientation relative to P23 promoter	This study
pIB4Q15	pIB184Km containing *S. gordonii* 0029 in orientation to P23 promoter	This study
pIB4Q22	pET3a containing SMU.2137 fused to a C-terminal 6×His tag	This study
pIB4Q24	pIB184Em containing SMU.2137 in orientation to P23 promoter	This study
pIB4Q25	pIB190 containing SMU.2137 in orientation to P23 promoter with N-terminal 6×His tag	This study
pIB4Q26	pIB184Km containing SMU.2137 in orientation to P23 promoter	This study
pIB4Q32	pIB184Km containing the SMU.2137 ORF with substitutions coding for RKR→AAA	This study
pIB4Q34	pIB184Km containing the frame-shifted SMU.2137 ORF with an altered start codon ATG→ATAG	This study
pIB4Q45	Derivative of pKT25 with *sprV* genetically fused in frame to T25 polypeptide; Km^r	This study
pIB4Q46	Derivative of pUT18 with *sprV* genetically fused in frame to T18 polypeptide; Ap^r	This study
pIB4Q47	Derivative of pUT18 with ribosomal protein S2 genetically fused in frame to T18 polypeptide; Ap^r	This study
pIB4Q48	Derivative of pUT18 with ribosomal protein L9 genetically fused in frame to T18 polypeptide; Ap^r	This study

primers, see Table S1 in the supplemental material), digested with BamHI/EcoRI, and ligated with pIB184Km, which was predigested with the same enzymes. The resulting construct was designated pIB4Q6. Similarly, the *sprV* homolog in *S. gordonii* was amplified using primers 4QSG0029CoF/4QSG0029CoR to include the 200-bp-long upstream elements and ligated with pIB184Km after digestion with BamHI/EcoRI. The resulting construct was named pIB4Q15. To express *sprV* under the control of the P23 promoter in pIB184Km, the *sprV* ORF was amplified using primers 4Q2137BamRBSF/4Q2137EcoR, digested with BamHI/EcoRI, and ligated with pIB184Km, which was digested with the same enzymes. This construct was designated pIB4Q26 and was subsequently used to introduce mutations in the *sprV* ORF. Plasmid pIB4Q26 was used as the template for long-range PCRs (using AccuTaq LA DNA polymerase; Sigma) with primers 4Q2137FS-F/4Q2137FS-R, which introduced a frameshift mutation in the start codon of the *sprV* ORF by changing ATG to ATAG, resulting in pIB4Q34. Similarly, the long-range PCR with primers 2137RKR-AAAF/2137RKR-AAAR, containing codon substitutions for R34A, K35A, and R36A (CGT→GCA, AAG→GCA, and CGT→GCA), generated construct pIB4Q32. To overexpress *S. mutans sprV* for protein purification, the *sprV* ORF was amplified with primers 4Q2137PET15F/4Q2137Ct6HisR, digested with NdeI/BamHI, and ligated to pET3a (Novagen), which was previously digested with the same enzymes. The resulting expression construct pIB4Q22 was used to obtain SprV with a C-terminal six-histidine tag (SprV-6×His). The bacterial adenylate cyclase two-hybrid system (Euromedex) was used to determine the interaction between SprV and its predicted interaction partners as recommended by the manufacturer. Vectors pKT25 and pUT18 were used to express bait and prey proteins by cloning respective ORFs in the BamHI and KpnI sites of these vectors. All plasmid constructs were verified by sequencing both strands. Strains and plasmids used in this study are listed in Table 2.

Biofilm formation. Biofilm formation was assessed in THY and in THY plus 1% sucrose as described earlier (40) with minor modifications. Briefly, overnight cultures of test strains were adjusted to an OD_{600}

of 0.2 with THY in the presence or absence of sucrose. Biofilms were grown in polystyrene 96-well flat-bottom plates by placing a 250-μl aliquot of the desired strain in each well. To grow biofilms on glass, 450-μl aliquots of the dilutions were placed in separate chambers of 8-well chamber slides. Biofilms were allowed to grow for 48 h at 37°C under microaerophilic conditions, after which they were washed, stained with Gram's crystal violet, washed, and imaged. False-colored surface plots of biofilm micrographs were generated using ImageJ (41).

Stress susceptibility assays. To test for stress sensitivity, strains to be tested were adjusted to the same densities in saline and serially diluted, after which a 10-μl aliquot from each dilution was spotted onto stressor plates and allowed to dry. Similar spots were also made on control plates with no stressors to assess normal bacterial growth. Plates were incubated at 37°C under microaerophilic conditions for up to 72 h to monitor for bacterial growth and then imaged. Acid stressor plates were prepared by adjusting the pH of THY agar to 5.5 with HCl. Additionally, the medium was buffered with citrate-phosphate buffer (pH 5.5) in order to maintain pH during bacterial growth as described earlier (42). Similarly, control plates for acid stress contained THY agar buffered at pH 7.5. Heat stress was induced by incubating THY plates spotted with serial dilutions of test strains at 42°C under microaerophilic conditions for 72 h, after which bacterial growth was monitored and imaged. Osmotic stressor plates contained THY agar supplemented with 0.5 M NaCl, and oxidative stressor plates contained THY agar containing either 1 mM H_2O_2 or 4 mM methyl viologen. UV sensitivity was determined by swabbing a line of each test culture across a THY agar plate, after which half of the petri dish was covered with a glass plate to block UV radiation and the agar plate was exposed to UV short-wave radiation (253.7 nm) for 15 s. Plates were then wrapped with aluminum foil and incubated at 37°C under microaerophilic conditions. The degree of sensitivity to antibiotics and stress-inducing agents was determined by disc diffusion assays as previously described (31), and the zone of growth inhibition was considered as the level of sensitivity.

SprV protein expression and purification. *E. coli* BL21(DE3) containing pIB4Q22 was grown to late log phase (OD_{600} = 0.6) at 37°C. The culture was then transferred to 16°C for 30 min, induced with 0.3 mM isopropyl-β-D-thiogalactopyranoside (IPTG), and allowed to express the recombinant protein for 16 h. Cells were harvested, washed with saline, and stored at −20°C. Cell pellets were lysed by ultrasonication in lysis buffer (50 mM Tris-Cl, 200 mM NaCl, 20 mM imidazole, and 5% glycerol at pH 7.5) containing a protease inhibitor cocktail (Sigma). Recombinant SprV-6×His was purified from the clarified lysate by affinity chromatography using Ni-nitrilotriacetic acid (NTA) resin by following the standard protocol. Purified proteins were dialyzed in a storage buffer (50 mM Tris-Cl, 200 mM NaCl, and 10% glycerol) before storage at −20°C.

RNA sequencing and data analysis. Total RNAs from exponential-growth-phase cultures of *S. mutans* UA159 and its isogenic *sprV* deletion mutant were prepared using the RNeasy kit (Qiagen) following the manufacturer's recommendations. Cell pellets were pretreated with the RNAprotect bacterial reagent to stabilize RNA. Prepared RNA was quantified spectrophotometrically and subjected to RNase-free DNase (Qiagen) treatment for 45 min. After removal of DNA, mRNA was enriched from the total RNA using the Ribo-Zero rRNA removal kit (Illumina) according to the manufacturer's recommendations. Resulting mRNA was quantified fluorometrically and subjected to the Illumina paired-end 100-bp library preparation protocols as per the manufacturer's recommendations. Prepared libraries were pooled at the equimolar ratio and sequenced on the high-output paired-end flow cell of a HiSeq 2500. Resulting reads were subjected to quality control (Sickle v1.200) (https://github.com/najoshi/sickle) and adapter contamination removal (Scythe v0.991) (https://github.com/vsbuffalo/scythe). High-quality, adapter-free reads were mapped onto the *S. mutans* chromosome (GenBank accession number NC_004350) using TopHat v2.0.10 (https://github.com/infphilo/tophat). Differentially expressed genes (DEGs) were identified using Cufflinks v2.2.1 (https://github.com/cole-trapnell-lab/cufflinks). A fold change threshold of 2 and a significance threshold q of $<$0.05 were applied, after which DEGs were manually classified into functional groups based on the KEGG database. This information was used to generate representative pie charts.

DNA uptake assays. The natural transformation efficiency of *S. mutans* was tested in the presence and absence of an extraneous competence-stimulating peptide. Overnight cultures of test strains were diluted 1/20 in fresh THY containing horse serum and allowed to grow at 37°C until exponential growth was achieved. To these cultures, competence-stimulating peptide (CSP-18) was added to a final concentration of 500 ng/ml wherever required, after which they were allowed to grow for another 30 min. To 1-ml aliquots of these cultures, 100 ng or 500 ng of pGhost9-TR, which confers resistance to erythromycin, was added and mixed well by pipetting. The mixture was incubated for 1 h at 37°C after which serial dilutions of each culture were spotted on THY agar and THY containing erythromycin to assess viability and transformation efficiency. Transformation efficiency of *S. gordonii* was assessed using a similar protocol but without the addition of CSP-18 and using the genomic DNA isolated from a spontaneous streptomycin-resistant derivative of *S. gordonii*.

Localization of SprV in *S. mutans*. Proteins from subcellular fractions of *S. mutans* were resolved by 12% SDS-PAGE using a Tris-Tricine buffer system. Resolved proteins were blotted on polyvinylidene difluoride (PVDF) membranes (Thermo Fisher), which were later blocked with 5% bovine serum albumin (BSA) prepared in Tris-buffered saline containing 0.1% Tween 20 (TBST). Blots were probed using an anti-SprV peptide antibody (GenScript) raised in rabbits as the primary antibody. Anti-rabbit IgG–horseradish peroxidase (HRP) conjugate (Thermo Fisher) was used as a secondary antibody. Washed blots were detected by overlaying them with the Pierce ECL Plus chemiluminescent assay substrate (Thermo Fisher). Purified SprV-6×His served as the positive control, while the Δ*sprV* strain served as the negative control. *S. mutans* cell pellets from 50 ml of culture were lysed by mechanical disruption with glass beads in 0.75 ml of lysis buffer (50 mM HEPES, 200 mM NaCl, and 5% glycerol at pH 7.5 with a protease inhibitor

cocktail [Sigma]) and clarified by centrifugation at 13,500 rpm for 20 min at 4°C to obtain the clarified cell lysate fraction. To the pellet fraction, 0.3 ml of 1× SDS loading dye was added, mixed well by pipetting, and heated to 100°C for 5 min. Cell wall fraction was obtained as described earlier (43). Cell surface proteins were obtained by incubating *S. mutans* cells as suspensions prepared in phosphate-buffered saline (PBS) containing a 0.2% *N*-dodecyl-*N*,*N*-dimethyl-3-ammonio-1-propanesulfonate (Zwittergent; Sigma) for 1 h as described earlier (33).

Cross complementation of an *E. coli hfq* deletion mutant with *sprV*. To determine whether SprV can functionally replace Hfq in *E. coli*, strains SG30013 and YN585 (44) were used as described earlier (45). SG30013 contains an *rpoS-lacZ* fusion, while YN585 is a derivative of SG30013 containing a *cat* insertion in the *hfq* gene. Briefly, *E. coli* YN585 strains containing appropriate vector controls (pIB190 and pIB184Em) and SprV expression plasmids (pIB4Q24 and pIB4Q25) were generated. Vector control plasmids were also transformed into strain SG30013. The resulting strains were streaked out on MacConkey agar and incubated at 37°C for 16 h to assess Hfq-dependent *rpoS-lacZ* expression. Expression of *rpoS-lacZ* (red colonies on MacConkey agar) indicated the presence of a functional Hfq or homologous protein.

SUPPLEMENTAL MATERIAL

Supplemental material for this article may be found at https://doi.org/10.1128/JB.00847-16.

SUPPLEMENTAL FILE 1, PDF file, 0.1 MB.

ACKNOWLEDGMENTS

RNA sequencing reported in this publication was made possible in part by the services of the KU Genome Sequencing Core Laboratory, which is supported by the National Institute of General Medical Sciences (NIGMS) (P20GM103638). This work was supported in part by National Institute of Dental and Craniofacial Research (NIDCR) research grants DE21664 and DE22660, awarded to I.B.

We thank Nadya Galeva (Mass Spectrometry Laboratory, University of Kansas) for identification of protein bands. We also thank Stuart MacDonald (K-INBRE Bioinformatics Core at the University of Kansas) for help with RNA sequencing data analysis. M.S. gratefully acknowledges constructive discussions and critical comments from members of the Biswas lab.

REFERENCES

1. Mitchell TJ. 2003. The pathogenesis of streptococcal infections: from tooth decay to meningitis. Nat Rev Microbiol 1:219–230. https://doi.org/10.1038/nrmicro771.
2. Biswas I, Drake L, Erkina D, Biswas S. 2008. Involvement of sensor kinases in the stress tolerance response of *Streptococcus mutans*. J Bacteriol 190:68–77. https://doi.org/10.1128/JB.00990-07.
3. Lemos JA, Burne RA. 2002. Regulation and physiological significance of ClpC and ClpP in *Streptococcus mutans*. J Bacteriol 184:6357–6366. https://doi.org/10.1128/JB.184.22.6357-6366.2002.
4. Mann B, van Opijnen T, Wang J, Obert C, Wang YD, Carter R, McGoldrick DJ, Ridout G, Camilli A, Tuomanen EI, Rosch JW. 2012. Control of virulence by small RNAs in *Streptococcus pneumoniae*. PLoS Pathog 8:e1002788. https://doi.org/10.1371/journal.ppat.1002788.
5. Storz G, Wolf YI, Ramamurthi KS. 2014. Small proteins can no longer be ignored. Annu Rev Biochem 83:753–777. https://doi.org/10.1146/annurev-biochem-070611-102400.
6. Hobbs EC, Fontaine F, Yin X, Storz G. 2011. An expanding universe of small proteins. Curr Opin Microbiol 14:167–173. https://doi.org/10.1016/j.mib.2011.01.007.
7. Yang X, Jensen SI, Wulff T, Harrison SJ, Long KS. 2016. Identification and validation of novel small proteins in *Pseudomonas putida*. Environ Microbiol Rep 8:966–974. https://doi.org/10.1111/1758-2229.12473.
8. Moller T, Franch T, Hojrup P, Keene DR, Bachinger HP, Brennan RG, Valentin-Hansen P. 2002. Hfq: a bacterial Sm-like protein that mediates RNA-RNA interaction. Mol Cell 9:23–30. https://doi.org/10.1016/S1097-2765(01)00436-1.
9. Vogel J, Luisi BF. 2011. Hfq and its constellation of RNA. Nat Rev Microbiol 9:578–589. https://doi.org/10.1038/nrmicro2615.
10. Lawhon SD, Frye JG, Suyemoto M, Porwollik S, McClelland M, Altier C. 2003. Global regulation by CsrA in *Salmonella* Typhimurium. Mol Microbiol 48:1633–1645. https://doi.org/10.1046/j.1365-2958.2003.03535.x.
11. Liu MY, Gui G, Wei B, Preston JF, III, Oakford L, Yuksel U, Giedroc DP, Romeo T. 1997. The RNA molecule CsrB binds to the global regulatory protein CsrA and antagonizes its activity in *Escherichia coli*. J Biol Chem 272:17502–17510. https://doi.org/10.1074/jbc.272.28.17502.
12. Karzai AW, Roche ED, Sauer RT. 2000. The SsrA-SmpB system for protein tagging, directed degradation and ribosome rescue. Nat Struct Biol 7:449–455. https://doi.org/10.1038/75843.
13. Wadler CS, Vanderpool CK. 2007. A dual function for a bacterial small RNA: SgrS performs base pairing-dependent regulation and encodes a functional polypeptide. Proc Natl Acad Sci U S A 104:20454–20459. https://doi.org/10.1073/pnas.0708102104.
14. Reizer J, Romano AH, Deutscher J. 1993. The role of phosphorylation of HPr, a phosphocarrier protein of the phosphotransferase system, in the regulation of carbon metabolism in Gram-positive bacteria. J Cell Biochem 51:19–24. https://doi.org/10.1002/jcb.240510105.
15. Ruvolo MV, Mach KE, Burkholder WF. 2006. Proteolysis of the replication checkpoint protein Sda is necessary for the efficient initiation of sporulation after transient replication stress in *Bacillus subtilis*. Mol Microbiol 60:1490–1508. https://doi.org/10.1111/j.1365-2958.2006.05167.x.
16. Gaballa A, Antelmann H, Aguilar C, Khakh SK, Song KB, Smaldone GT, Helmann JD. 2008. The *Bacillus subtilis* iron-sparing response is mediated by a Fur-regulated small RNA and three small, basic proteins. Proc Natl Acad Sci U S A 105:11927–11932. https://doi.org/10.1073/pnas.0711752105.
17. Biswas I, Mohapatra SS. 2012. CovR alleviates transcriptional silencing by a nucleoid-associated histone-like protein in *Streptococcus mutans*. J Bacteriol 194:2050–2061. https://doi.org/10.1128/JB.06812-11.
18. Singh K, Senadheera DB, Levesque CM, Cvitkovitch DG. 2015. The *copYAZ* operon functions in copper efflux, biofilm formation, genetic transformation, and stress tolerance in *Streptococcus mutans*. J Bacteriol 197:2545–2557. https://doi.org/10.1128/JB.02433-14.
19. Hossain MS. 2012. Mutacin IV production in *Streptococcus mutans*

UA159: characterization, regulation, and mechanism of self-immunity. PhD thesis. University of Kansas, Lawrence, KS.
20. Taboada B, Ciria R, Martinez-Guerrero CE, Merino E. 2012. ProOpDB: Prokaryotic Operon DataBase. Nucleic Acids Res 40:D627–D631. https://doi.org/10.1093/nar/gkr1020.
21. Wang L, Brown SJ. 2006. BindN: a web-based tool for efficient prediction of DNA and RNA binding sites in amino acid sequences. Nucleic Acids Res 34:W243–W248. https://doi.org/10.1093/nar/gkl298.
22. Meier M, Sit RV, Quake SR. 2013. Proteome-wide protein interaction measurements of bacterial proteins of unknown function. Proc Natl Acad Sci U S A 110:477–482. https://doi.org/10.1073/pnas.1210634110.
23. Lei Y, Oshima T, Ogasawara N, Ishikawa S. 2013. Functional analysis of the protein Veg, which stimulates biofilm formation in *Bacillus subtilis*. J Bacteriol 195:1697–1705. https://doi.org/10.1128/JB.02201-12.
24. Li YH, Tang N, Aspiras MB, Lau PC, Lee JH, Ellen RP, Cvitkovitch DG. 2002. A quorum-sensing signaling system essential for genetic competence in *Streptococcus mutans* is involved in biofilm formation. J Bacteriol 184:2699–2708. https://doi.org/10.1128/JB.184.10.2699-2708.2002.
25. Senadheera MD, Guggenheim B, Spatafora GA, Huang YC, Choi J, Hung DC, Treglown JS, Goodman SD, Ellen RP, Cvitkovitch DG. 2005. A VicRK signal transduction system in *Streptococcus mutans* affects *gtfBCD*, *gbpB*, and *ftf* expression, biofilm formation, and genetic competence development. J Bacteriol 187:4064–4076. https://doi.org/10.1128/JB.187.12.4064-4076.2005.
26. Wen ZT, Baker HV, Burne RA. 2006. Influence of BrpA on critical virulence attributes of *Streptococcus mutans*. J Bacteriol 188:2983–2992. https://doi.org/10.1128/JB.188.8.2983-2992.2006.
27. van der Ploeg JR. 2005. Regulation of bacteriocin production in *Streptococcus mutans* by the quorum-sensing system required for development of genetic competence. J Bacteriol 187:3980–3989. https://doi.org/10.1128/JB.187.12.3980-3989.2005.
28. Deng DM, Liu MJ, ten Cate JM, Crielaard W. 2007. The VicRK system of *Streptococcus mutans* responds to oxidative stress. J Dent Res 86:606–610. https://doi.org/10.1177/154405910708600705.
29. Ahn SJ, Wen ZT, Burne RA. 2006. Multilevel control of competence development and stress tolerance in *Streptococcus mutans* UA159. Infect Immun 74:1631–1642. https://doi.org/10.1128/IAI.74.3.1631-1642.2006.
30. Lemos JA, Chen YY, Burne RA. 2001. Genetic and physiologic analysis of the *groE* operon and role of the HrcA repressor in stress gene regulation and acid tolerance in *Streptococcus mutans*. J Bacteriol 183:6074–6084. https://doi.org/10.1128/JB.183.20.6074-6084.2001.
31. Chattoraj P, Banerjee A, Biswas S, Biswas I. 2010. ClpP of *Streptococcus mutans* differentially regulates expression of genomic islands, mutacin production, and antibiotic tolerance. J Bacteriol 192:1312–1323. https://doi.org/10.1128/JB.01350-09.
32. Fukushima T, Ishikawa S, Yamamoto H, Ogasawara N, Sekiguchi J. 2003. Transcriptional, functional and cytochemical analyses of the *veg* gene in *Bacillus subtilis*. J Biochem 133:475–483. https://doi.org/10.1093/jb/mvg062.
33. Wilkins JC, Beighton D, Homer KA. 2003. Effect of acidic pH on expression of surface-associated proteins of *Streptococcus oralis*. Appl Environ Microbiol 69:5290–5296. https://doi.org/10.1128/AEM.69.9.5290-5296.2003.
34. Chao Y, Vogel J. 2010. The role of Hfq in bacterial pathogens. Curr Opin Microbiol 13:24–33. https://doi.org/10.1016/j.mib.2010.01.001.
35. Christiansen JK, Larsen MH, Ingmer H, Sogaard-Andersen L, Kallipolitis BH. 2004. The RNA-binding protein Hfq of *Listeria monocytogenes*: role in stress tolerance and virulence. J Bacteriol 186:3355–3362. https://doi.org/10.1128/JB.186.11.3355-3362.2004.
36. Bohn C, Rigoulay C, Bouloc P. 2007. No detectable effect of RNA-binding protein Hfq absence in *Staphylococcus aureus*. BMC Microbiol 7:10. https://doi.org/10.1186/1471-2180-7-10.
37. Brennan RG, Link TM. 2007. Hfq structure, function and ligand binding. Curr Opin Microbiol 10:125–133. https://doi.org/10.1016/j.mib.2007.03.015.
38. Banerjee A, Biswas I. 2008. Markerless multiple-gene-deletion system for *Streptococcus mutans*. Appl Environ Microbiol 74:2037–2042. https://doi.org/10.1128/AEM.02346-07.
39. Biswas I, Jha JK, Fromm N. 2008. Shuttle expression plasmids for genetic studies in *Streptococcus mutans*. Microbiology 154:2275–2282. https://doi.org/10.1099/mic.0.2008/019265-0.
40. Biswas S, Biswas I. 2005. Role of HtrA in surface protein expression and biofilm formation by *Streptococcus mutans*. Infect Immun 73:6923–6934. https://doi.org/10.1128/IAI.73.10.6923-6934.2005.
41. Schneider CA, Rasband WS, Eliceiri KW. 2012. NIH Image to ImageJ: 25 years of image analysis. Nat Methods 9:671–675. https://doi.org/10.1038/nmeth.2089.
42. Krol JE, Biswas S, King C, Biswas I. 2014. SMU.746-SMU.747, a putative membrane permease complex, is involved in aciduricity, acidogenesis, and biofilm formation in *Streptococcus mutans*. J Bacteriol 196:129–139. https://doi.org/10.1128/JB.00960-13.
43. Siegel JL, Hurst SF, Liberman ES, Coleman SE, Bleiweis AS. 1981. Mutanolysin-induced spheroplasts of *Streptococcus mutants* are true protoplasts. Infect Immun 31:808–815.
44. Wassarman KM, Repoila F, Rosenow C, Storz G, Gottesman S. 2001. Identification of novel small RNAs using comparative genomics and microarrays. Genes Dev 15:1637–1651. https://doi.org/10.1101/gad.901001.
45. Vrentas C, Ghirlando R, Keefer A, Hu Z, Tomczak A, Gittis AG, Murthi A, Garboczi DN, Gottesman S, Leppla SH. 2015. Hfqs in *Bacillus anthracis*: role of protein sequence variation in the structure and function of proteins in the Hfq family. Protein Sci 24:1808–1819. https://doi.org/10.1002/pro.2773.
46. Ajdic D, McShan WM, McLaughlin RE, Savic G, Chang J, Carson MB, Primeaux C, Tian R, Kenton S, Jia H, Lin S, Qian Y, Li S, Zhu H, Najar F, Lai H, White J, Roe BA, Ferretti JJ. 2002. Genome sequence of *Streptococcus mutans* UA159, a cariogenic dental pathogen. Proc Natl Acad Sci U S A 99:14434–14439. https://doi.org/10.1073/pnas.172501299.
47. Kolenbrander PE, Andersen RN, Moore LV. 1990. Intrageneric coaggregation among strains of human oral bacteria: potential role in primary colonization of the tooth surface. Appl Environ Microbiol 56:3890–3894.
48. Karimova G, Pidoux J, Ullmann A, Ladant D. 1998. A bacterial two-hybrid system based on a reconstituted signal transduction pathway. Proc Natl Acad Sci U S A 95:5752–5756. https://doi.org/10.1073/pnas.95.10.5752.